Phenomenological theory of the kink instability in a slender plasma column

D. D. Ryutov[a)]
Lawrence Livermore National Laboratory, Livermore, California 94551

I. Furno, T. P. Intrator, S. Abbate, and T. Madziwa-Nussinov
Los Alamos National Laboratory, Los Alamos, New Mexico 87545

(Received 23 November 2005; accepted 6 February 2006; published online 29 March 2006)

In this paper we are concerned with the kink instability of a current-carrying plasma column whose radius a is much smaller than its length L. In the limit $a \ll L$, one can consider the column as a thin filament whose kinking can be adequately described simply by a two dimensional 2D displacement vector, $\xi_x = \xi_x(z,t)$; $\xi_y = \xi_y(z,t)$. Details of the internal structure of the column such as the radial distribution of the current, density, and axial flow can be lumped into some phenomenological parameters. This approach is particularly efficient in the problems with nonideal (sheath) boundary conditions (BC) at the end electrodes, with the finite plasma resistivity, and with a substantial axial flow. With the sheath BC imposed at one of the endplates, we find instability in the domain well below the classical Kruskal-Shafranov limit. The presence of an axial flow causes the onset of rotation of the kink and strong axial "skewness" of the eigenfunction, with the perturbation amplitude increasing in the flow direction. The limitations of the phenomenological approach are analyzed and are related to the steepness with which the plasma resistivity increases at the plasma boundary with vacuum. © *2006 American Institute of Physics*. [DOI: 10.1063/1.2180667]

I. INTRODUCTION

The screw pinch is a magnetic configuration that has been studied for decades, in conjunction with fusion research, astrophysical problems, and basic plasma physics. One of the most salient features of screw pinches is the development of the $m=1$ global kink mode, which was a subject of numerous theoretical and experimental studies. We can refer the reader to the textbook[1] and recent publications,[2–5] where further references can also be found. The role of this instability in the context of Solar Physics has been discussed in a general survey.[6]

In this study, we suggest a simplified description of a pinch with a length L much exceeding its radius a. What is new in our study compared to the most recent theoretical analyses of the similar problem[4,5] is that we suggest a unified way for describing such effects as boundary conditions at the electrodes (including the sheaths), finite plasma resistivity, and plasma axial flow. We call our approach "phenomenological" because it includes some ad hoc assumptions, which, although having a clear physical meaning, can be justified only in a qualitative way. This leads to the appearance of some parameters whose exact value can be found only from fitting the theory predictions and the experimental data.

Our approach is heavily based on the use of the inequality $a \ll L$. In this case, when becoming unstable, the $m=1$ mode causes only "gentle" wiggling of the column, so that the angle formed by the column with its unperturbed direction remains small. We do not consider here the situation where the plasma current would exceed the Kruskal-Shafranov current by a large margin, thereby bringing the column to the state of a violent motion and even complete disruption: we are concerned only with the states that are moderately overcritical.

We use Cartesian coordinates with the axis z coinciding with the unperturbed axis of the column and the origin situated at the lower endplate (Fig. 1). Occasionally we use also cylindrical coordinates, with the azimuthal angle θ measured from the axis x. We describe the deformation of the column as a result of small translation of every cross section in the x-y plane (Fig. 2), and neglect any deformation of the cross section, so that every cross section is merely translated in the x-y plane.

One can find a justification for this assumption in that, experimentally, the flux ropes demonstrate a remarkable cohesiveness.[2,3] The theory justification can be found for the case where viscous and/or gyroviscous effects[7] are important and slow down any deformations of the cross section. The model of the "rigid" cross sections was successfully used in the analysis of the mirror stability.[8] We do not try here to provide any deeper assessment of possible deviations from this approximation. This is yet another sign of the phenomenological nature of our approach.

Within this model the shape of the deformed column can be described by the function

$$\boldsymbol{\xi} = \boldsymbol{\xi}(z,t), \tag{1}$$

which is a two-dimensional vector of a transverse displacement of the column with respect to its unperturbed position. The condition that the deformations are "gentle" can be formulated as

$$\left| \frac{\partial \boldsymbol{\xi}}{\partial z} \right| \ll 1. \tag{2}$$

[a)]Author to whom correspondence should be addressed. Electronic mail: ryutov1@llnl.gov

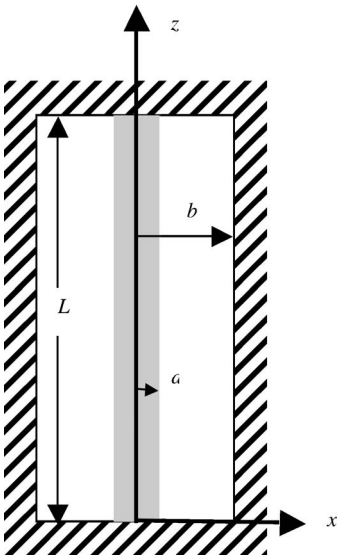

FIG. 1. The geometry of the problem. The axis y is directed away from the reader.

The description in terms of a single 2D vector function is a key ingredient of our approach: we do not consider the internal structure of the column, only its overall shape, as determined by the displacement of circular cross sections in the x and y directions, Fig. 2.

These assumptions mean that we cannot analyze the internal dynamics of the column, in particular, internal kinks. Our model is suitable only for considering global external kinks. The inner structure of the unperturbed column, e.g., the radial distribution of temperature and density, will be included into our model in the form of lumped phenomenological coefficients. An approach that we use to implement this program is described in the subsequent sections.

II. THE GEOMETRY AND BASIC ORDERING

The geometry is illustrated by Fig. 1. With regard to the radius of the return current conductor b, we assume that it satisfies an inequality,

$$a \ll b. \tag{3}$$

Under such conditions, b drops out from the analysis.[4] (Our approach can, however, be easily extended to the case where b becomes close to a, but both are still considerably smaller than L.)

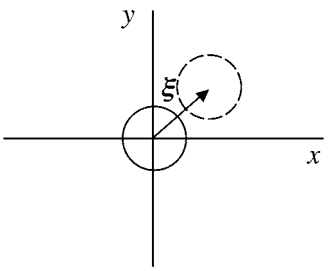

FIG. 2. Deformation of the column. The axis z is directed toward the reader. The solid line represents the initial cross section, whereas the dashed line shows a displaced cross section. In each cross section z=const, the displacement vector $\boldsymbol{\xi}$ is the same for all initial points (a rigid displacement).

As mentioned in the Introduction, we consider perturbations that can be characterized by the "rigid" displacements of the "slices" of the plasma column in the x-y planes:

$$\xi_x = \xi_x(z,t), \quad \xi_y = \xi_y(z,t), \tag{4}$$

Fig. 2. This is a good approximation for a long-wavelength $m=1$ mode under condition (3). The axial magnetic field is large compared to the azimuthal magnetic field,

$$B_\theta / B_z \sim a/L \ll 1. \tag{5}$$

This corresponds to the standard scaling for the kink mode.

The plasma pressure is assumed to be small compared to the magnetic pressure, so that the axial magnetic field is almost uniform. On the other hand, the finite plasma pressure does not have any dramatic direct effect on the current-driven global kinks. So, one can expect that our results will be at least qualitatively correct, even at $\beta \sim 1$.

We start from the simplest model of a perfectly conducting, initially resting plasma. Later on, we add effects related to the plasma axial flow and finite plasma resistivity.

The plasma radius a is defined by the condition that the conductivity outside this radius is negligibly small, and the external region can be considered as a vacuum. Setting this boundary is an important step. When deforming the column in a way indicated by Eq. (4), we bend the bundle of magnetic field lines frozen into the plasma and perturb also an external axial field, thereby creating a restoring force. This force increases as the bundle of bent field lines becomes thicker, i.e., the bending stiffness grows with the bundle radius a. In particular, this is reflected by the fact that the "standard" Kruskal-Shafranov criterion[9,10] for the critical current reads as

$$I_{ks} = \frac{\pi a^2 B_z c}{L} = \frac{c\Phi}{L}, \tag{6}$$

where c is the speed of light, and Φ is a flux of the axial magnetic field through the plasma column cross section. We use the CGS (Gaussian) system of units. For the perturbations of the type (4) the plasma boundary is not the boundary that contains, say, 90% of the plasma mass; it is rather the boundary beyond which the conductivity becomes low. So, there is some uncertainty in the definition of a, and this is one of the manifestations of the phenomenological nature of our model, as outlined in the Introduction. Figure 3 illustrates this point with example profiles for density, current density, and conductivity.

III. THE CASE OF A ZERO FLOW

A. Basic equations

The forces acting on the plasma column can be evaluated by using the energy principle. In a long-thin approximation, this has been done in a number of papers, in particular, in Refs. 4, 5, and 11. As a result, one obtains the following equations of motion:

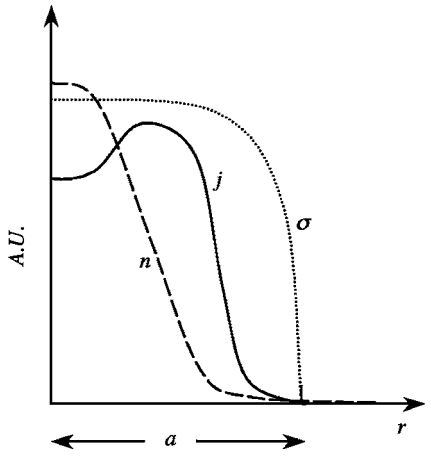

FIG. 3. A sketch of the current density distribution (solid line), the density distribution (dashed line), and the electrical conductivity distribution (dotted line). As the plasma conductivity depends only on the plasma temperature, the current profile may be broader than the density profile—for a uniform temperature. The current would drop in the zone where the density is so small that the standard model of the plasma conductivity does not work. In the figure, a particular case of a hollow current profile is shown, but our analysis is applicable to an arbitrary distribution. The parameter a that enters our equations is determined by the condition that, at $r<a$, the conductivity is high enough to make the axial magnetic field to be frozen into the plasma. Therefore, a depends on the frequency of perturbations. However, for a steep-enough decrease of the electrical conductivity, a is well defined.

$$\bar{\rho}\frac{\partial^2 \xi_x}{\partial t^2} = \frac{B_z^2}{2\pi}\frac{\partial^2 \xi_x}{\partial z^2} - \frac{B_z B_\theta}{2\pi a}\frac{\partial \xi_y}{\partial z},$$

$$\bar{\rho}\frac{\partial^2 \xi_y}{\partial t^2} = \frac{B_z^2}{2\pi}\frac{\partial^2 \xi_y}{\partial z^2} + \frac{B_z B_\theta}{2\pi a}\frac{\partial \xi_x}{\partial z}. \tag{7}$$

Here B_θ is evaluated at the plasma boundary. The definition of the average density is

$$\bar{\rho} = \frac{2}{a^2}\int_0^a \rho r\, dr. \tag{8}$$

The first term on the right-hand side (rhs) of Eq. (7) is related to the restoring force associated with the perturbation of the axial magnetic field both inside and outside the plasma column. [When no axial current is present, Eq. (7) describes the shear Alfvén wave propagating along the column.] The second term accounts for the destabilizing interaction of the axial current with the axial magnetic field.

By introducing a complex displacement,

$$\eta = \xi_x + i\xi_y, \tag{9}$$

one can reduce set (7) to a single equation:

$$\frac{\partial^2 \eta}{\partial t^2} = v_A^2\left(\frac{\partial^2 \eta}{\partial z^2} + ik_0\frac{\partial \eta}{\partial z}\right), \tag{10}$$

where

$$k_0 = \frac{B_\theta}{aB_z}, \tag{11}$$

and

$$v_A \equiv B_z/\sqrt{2\pi\bar{\rho}}. \tag{12}$$

The Alfvén velocity has been increased by $2^{1/2}$ with respect to the standard definition: this allows one to eliminate the appearance of additional numerical factors in the further equations. For the perturbation of the form of $\exp(-i\omega t)$, one obtains

$$-\omega^2\eta = v_A^2(\eta'' + ik_0\eta'), \tag{13}$$

where the prime denotes the differentiation over z.

We assume that the electrode situated at $z=0$ is perfectly conducting. This yields the following boundary condition (BC) at $z=0$:

$$\eta|_{z=0} = 0. \tag{14}$$

On the other hand, at this point, we do not make any assumptions about the BC at $z=L$. In what follows, we implement various BCs at $z=L$. It is actually not very difficult to impose an arbitrary BC at $z=0$ as well. However, this makes all the equations longer, without providing any new insights.

The eigenvalue problem described by Eqs. (13) and (14), and by some (as yet unspecified) BC at $z=L$, generally speaking, does not possess the property of self-adjointness; in particular, the square of the eigenfrequency ω^2 is not necessarily a real number. To identify the cases where the problem is self-adjoint, it is convenient to introduce a new unknown function,

$$\tilde{\eta} = \eta\exp(ik_0 z/2). \tag{15}$$

It satisfies the equation

$$-\omega^2\tilde{\eta} = v_A^2\left(\tilde{\eta}'' + \frac{k_0^2}{4}\tilde{\eta}\right), \tag{16}$$

with real coefficients on the right-hand side (rhs). Multiplying this equation by $\tilde{\eta}^*$ (where the asterisk denotes the complex conjugate), integrating over z, and accounting for the boundary condition (14), one finds

$$\omega^2\int_0^L |\tilde{\eta}|^2\, dz = v_A^2\int_0^L \left|\frac{\partial\tilde{\eta}}{\partial z}\right|^2 dz - \frac{k_0^2}{4}\int_0^L |\tilde{\eta}|^2\, dz - \left(\tilde{\eta}^*\frac{\partial\tilde{\eta}}{\partial z}\right)\Bigg|_{z=L}. \tag{17}$$

One sees that the system has a property of being self-adjoint if, at $z=L$, one of the following conditions holds: $\tilde{\eta}=0$ or $\partial\tilde{\eta}/\partial z=0$. If this is the case, the eigenfrequency is automatically either purely real (oscillations) or purely imaginary (exponential growth or decay). In other words, in these two cases one recovers the standard results of the energy principle.[12] The first boundary condition corresponds to a perfect line tying, whereas the second one can be considered a boundary condition on the poorly conducting surface (free sliding of the flux tube over the end surface). We will discuss this second boundary condition in more detail in Sec III C.

If formulated in terms of the initial unknown function η, these boundary conditions read as

$$\eta_{z=L} = 0 \tag{18}$$

and

$$\left(\frac{\partial \eta}{\partial z}+\frac{ik_0}{2}\eta\right)\Bigg|_{z=L}=0. \tag{19}$$

The solution of Eq. (13) is

$$\eta = C_1 e^{ik_1 z} + C_2 e^{ik_2 z}, \tag{20}$$

where

$$k_{1,2} = -\frac{k_0}{2} \pm \sqrt{\frac{k_0^2}{4}+\frac{\omega^2}{v_A^2}}. \tag{21}$$

Imposing the boundary condition of zero displacement at the surface $z=0$ [Eq. (14)], we find from Eq. (20) that $C_1 = -C_2 = C$, i.e.,

$$\eta = C\left(e^{ik_1 z} - e^{ik_2 z}\right), \tag{22}$$

where C is an arbitrary normalization constant. Here we have not made any assumptions regarding the boundary condition at the other endplate.

For the normalization $C=1/2$ that we use throughout this paper, one has from Eq. (22),

$$\xi_x = \frac{1}{2}\left(\cos k_1 z - \cos k_2 z\right),$$

$$\xi_y = \frac{1}{2}\left(\sin k_1 z - \sin k_2 z\right). \tag{23}$$

As will become clear later, this representation remains correct for a much broader set of the input parameters, e.g., for the case where the axial flow is included. What changes from case to case are specific expressions for k_1 and k_2.

B. Line tying at $z=L$

For the case where there is a perfect line tying at $z=L$, i.e., Eq. (18) holds, one has from Eq. (22),

$$k_1 - k_2 = \frac{2n\pi}{L}, \tag{24}$$

where $n=1,2,\ldots$, is an axial mode number. From Eqs. (21) and (23), one finds that

$$\frac{\omega^2}{v_A^2} = \frac{n^2\pi^2}{L^2} - \frac{k_0^2}{4}. \tag{25}$$

It is obvious that the most unstable mode corresponds to $n=1$. For this mode the critical current is equal to the Kruskal-Shafranov current I_{KS} (6). Note that, at the stability boundary, the eigenfunction is $\eta = C(1-e^{-ik_0 z})$, i.e., it is a superposition of the helical perturbation (the second term) and a pure translation perpendicular to the pinch axis (the first term). At higher currents, the growth rate is

$$\mathrm{Im}\ \omega = \frac{\pi v_A}{L}\sqrt{\frac{I^2}{I_{KS}^2}-1}. \tag{26}$$

In the example that we are considering now where both electrodes are perfectly conducting, we have, from Eqs. (21) and (24), with $n=1$, that

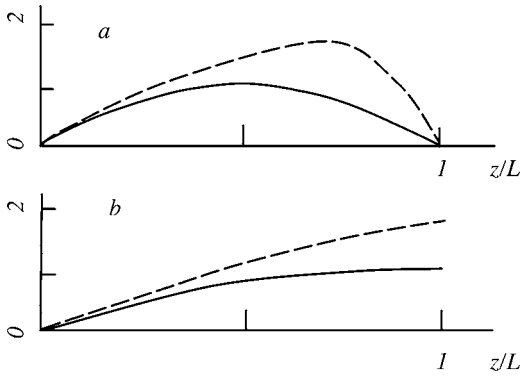

FIG. 4. The shape of the figure of revolution over which the axis of the plasma column is wound: (a) Line tying at both $z=0$ and $z=L$; the solid curve corresponds to the case of no axial flow; the dashed curve corresponds to the axial flow directed from $z=0$ to $z=L$, and to an overcritical situation. (b) Line tying at $z=0$, no line tying at $z=L$; the solid curve corresponds to the case of no flow and to a marginally stable case in the presence of the flow; the dashed curve corresponds to a somewhat supercritical system in the presence of the flow. The flow causes the advection of perturbations and causes a "skewing" of the eigenfunction in the direction of the $z=L$ electrode.

$$k_1 = \frac{\pi}{L} - \frac{k_0}{2}, \quad k_2 = -\frac{\pi}{L} - \frac{k_0}{2}. \tag{27}$$

From Eq. (23), we find that the perturbed axis of the column forms a helix wound over the axisymmetric surface with a radius

$$R \equiv \sqrt{\xi_x^2 + \xi_y^2} = \sin\frac{\pi z}{L} \tag{28}$$

(Fig. 4). For the linear stage of the instability, this result remains valid for any currents exceeding the critical current. As k_1 and k_2 are different, the pitch of the helix, generally speaking, changes over the length. So, generally speaking, it is incorrect to describe the perturbation as a perturbation with a constant pitch.

The next axial mode, $n=2$, has a critical current equal to $2I_{KS}$. One can therefore expect that, at $I<2I_{KS}$, the structure of the perturbation will be defined by Eq. (22); the saturated amplitude could, of course, be determined only by means of the nonlinear analysis (which is not a subject of this paper).

C. Perfect sliding of the flux tube at $z=L$

Now we consider the other "ideal" boundary condition, that described by Eq. (19). We can still use Eq. (22). When we impose boundary conditions [(14) at $z=0$ and (19) at $z=L$], we find

$$\exp i\left(k_1 - k_2\right)L = \frac{2k_2 + k_0}{2k_1 + k_0}. \tag{29}$$

Substituting $k_{1,2}$ from Eq. (21), we find

$$\exp i\left(k_1 - k_2\right)L = -1, \tag{30}$$

so that

$$k_1 - k_2 = \frac{n\pi}{L}. \tag{31}$$

Note that, compared to Eq. (23), the rhs is by a factor of 2 lower, signifying a lower instability threshold. For the most unstable mode (n=1), the critical current is equal to a half the Kruskal-Shafranov current. For higher currents, the growth rate is

$$\mathrm{Im}\ \omega = \frac{\pi v_A}{L}\sqrt{\frac{I^2}{I_{KS}^2} - \frac{1}{4}}. \tag{32}$$

The shape of the surface on which the axis of the plasma column is wound is now

$$R = \sin\frac{\pi z}{2L}, \tag{33}$$

both for critical and supercritical current [Fig. 4(b)]. The critical current for the $n=2$ mode is equal to I_{KS}.

We should note that the boundary condition (19) is different from the boundary condition

$$\left.\frac{\partial \eta}{\partial z}\right|_{z=L} = 0 \tag{34}$$

that one might invoke by the analogy with the oscillation of the rod with the free end. As condition (34) is of some conceptual interest, we discuss here the dispersion relation that stems from it.

By substituting solution (22) into Eq. (34) and using Eq. (21) for $k_{1,2}$, one obtains

$$\tan\left(L\sqrt{\frac{k_0^2}{4} + \frac{\omega^2}{v_A^2}}\right) = -\frac{2i}{k_0}\sqrt{\frac{k_0^2}{4} + \frac{\omega^2}{v_A^2}}. \tag{35}$$

This equation has an unstable solution, even at small k_0 ($k_0 \ll \pi/L$). In the limit of small k_0, the solution of Eq. (35) for the lowest axial mode is

$$\omega \approx \pm\frac{\pi v_A}{2L}\left(1 - \frac{2ik_0L}{\pi^2}\right). \tag{36}$$

Obviously, one of the roots is unstable. Note the definition (12) of v_A.

D. Sheath boundary conditions

1. Sheath current-voltage characteristics

Thus far, we have been considering only the cases where "ideal" boundary conditions of either perfect line tying or perfect sliding are imposed at the $z=L$ plane. In this section, we provide a qualitative phenomenological assessment of boundary conditions associated with the presence of a Debye sheath near the $z=L$ electrode.

We use the standard expression[13] for the z component of the current (assuming that axial magnetic field is much greater than the azimuthal one):

$$j_z = en\left(u - v_{Te}e^{-e\varphi/T_e}\right). \tag{37}$$

Here u is the ion flow velocity (of order of the ion sound speed), n is the particle density, T_e is the electron temperature, and φ is the potential at the plasma side of the sheath with respect to the plate potential. The plate itself is considered a good conductor, with the potential on the surface of the plate constant over the plate surface. In the unperturbed state, the current through the sheath is sustained by the externally applied voltage. Note that the role of the sheath resistance in the problems of the plasma stability has been recognized many years ago.[14,15]

When the magnetic field in the plasma is perturbed, then the perturbation of the z component of the current is generated. By virtue of Eq. (37), this leads to the perturbation of the sheath potential. The latter means that, at the plasma side of the sheath, the tangential electric field appears, despite the fact that the underlying surface is perfectly conducting.[16] The presence of the tangential electric field in the plasma means that the lateral displacements of the plasma column now become possible, i.e., the condition of a zero lateral displacement (perfect line tying) has to be replaced by a more general condition, which we derive in the next two subsections.

By perturbing Eq. (37), we find

$$\delta j_z = \alpha_1 enu\frac{e\,\delta\varphi}{T_e}, \tag{38}$$

where α_1 is a numerical factor of order one:

$$\alpha_1 = \frac{enu - j_0}{enu}, \tag{39}$$

and j_0 is the unperturbed current density. We assume that j_0 does not exceed the ion saturation current, so that $\alpha_1 > 0$.

2. Current density perturbation

To formulate the boundary condition, we need to express δj_z in terms of $\boldsymbol{\xi}(z)$. As will become clear from the discussion of this section, there are two sources for the axial current perturbation: the tilt ($\partial\boldsymbol{\xi}/\partial z$) and the shift ($\boldsymbol{\xi}$) of the column. For linear perturbations, their contributions can be considered separately and then superposed. Consider first the tilt of the column, assuming as everywhere else in this paper that $ka \ll 1$. For the perturbations with $ka \ll 1$, one can always choose a segment of the tube of a length Δz that satisfies a condition $a \ll \Delta z \ll 1/k$. The tilt of such a segment can be considered just as a tilt of a thin ($a \ll \Delta z$) cylindrical rod. If viewed in the frame attached to the rod, the external magnetic field gets tilted and acquires a component perpendicular to the axis of the rod. The component parallel to the rod axis, in the linear approximation, remains unchanged.

The appearance of the perpendicular magnetic field gives rise to the appearance of axial currents. In the case of a perfectly conducting rod, the structure of the magnetic field and distribution of the axial current are such as shown in Fig. 5(a). This figure corresponds to the column tilt in the x-z plane. At large distances from the rod, the magnetic field perturbation is uniform and has only the x component:

$$\delta B_{\perp y}|_{r\to\infty} = 0; \quad \delta B_{\perp x}|_{r\to\infty} = -B_z\frac{\partial \xi_x}{\partial z}. \tag{40}$$

As there are no currents outside the rod, $\delta\boldsymbol{B}_\perp$ can be presented there as a gradient of some scalar χ, $\delta\boldsymbol{B}_\perp = -\boldsymbol{\nabla}\chi$, with χ satisfying the equation $\nabla_\perp^2\chi = 0$. The normal component of

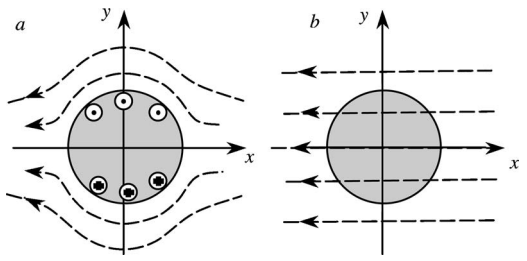

FIG. 5. The perturbation of the external magnetic field (in the rod frame) for the tilt in the x-z plane. The initial axial magnetic field B_z is positive; the tilt is also positive, $\partial\xi_x/\partial z>0$. The left panel corresponds to a perfectly conducting plasma; the dots (crosses) correspond to the surface current flowing toward (away from) the observer. The right panel corresponds to an opposite case of a very small conductivity, when the external field freely penetrates to the plasma. In the latter case the magnetic field in the laboratory frame remains unperturbed.

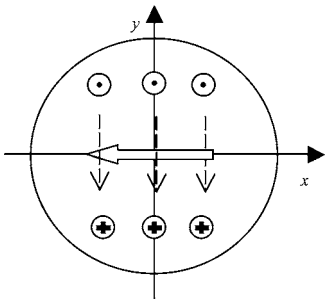

FIG. 6. Sheath reaction to the tilt of the column. The tilt occurs in the x direction, generating the perturbation of the z component of the current; the direction of the current is indicated by the circles with the dots (toward the viewer) and crosses (away from the viewer). The sheath resistance then leads to the formation of the electric field on the plasma side of the sheath; this field is directed along the dashed arrows. The presence of the field in the laboratory frame leads to the plasma drift in the direction of the block arrow.

the magnetic field must vanish at the surface of a perfectly conducting cylinder. The corresponding solution for the magnetic field in the cylindrical coordinates reads as

$$\delta B_r = -B_z \frac{\partial \xi_x}{\partial z}\cos\theta\left(1-\frac{a^2}{r^2}\right);$$
$$\delta B_\theta = B_z \frac{\partial \xi_x}{\partial z}\sin\theta\left(1+\frac{a^2}{r^2}\right). \tag{41}$$

As the tangential component of the magnetic field experiences a jump at the surface of the perfectly conducting cylinder, an axial surface current appears, with the linear current density (current per unit length of a circumference) equal to

$$\delta J_z = \frac{c}{4\pi}\delta B_\theta|_{r=a} = \frac{c}{2\pi}B_z\frac{\partial \xi_x}{\partial z}\sin\theta. \tag{42}$$

The current distribution is illustrated in Fig. 5(a).

In the case of a finite plasma resistivity, this current perturbation is spread over a fraction of the column radius. (The details of the radial distribution of the current density is determined by the radial distribution of the electrical conductivity.) Then, the current density perturbation can be presented as $\delta j_z=\alpha_2(cB_z/4\pi a)(\partial\xi_x/\partial z)\sin\theta$, where α_2 is a numerical coefficient of an order of a few that accounts for the radial extent of the current density distribution. For the tilt in the y-z plane, the expression for the current perturbation will have the same structure, with ξ_x replaced by ξ_y, and $\sin\theta$ replaced by $-\cos\theta$.

Consider now the current perturbation associated with the shift of the plasma column. This perturbation is a result of a mere translation in the x-y plane, and the current perturbation (for the displacement in the y direction) is simply $\delta j_z=-(\partial j_0/\partial r)\xi_y\sin\theta$ (and similarly for the displacement in the x direction, but with replacement of ξ_y by ξ_x, and $\sin\theta$ by $\cos\theta$). As $j_0\sim cB_\theta/2\pi a$, and B_θ is related to B_z by Eq. (11), we find that the part of the current perturbation associated with the displacement ξ_y can be presented as $\delta j_z=\alpha_3(cB_z/4\pi a)k_0\xi_y\sin\theta$ with α_3 being a coefficient of order 1 (for a smooth, bell-shaped distribution of the unperturbed current density). The total $\sin\theta$-dependent current perturbation is therefore

$$\delta j_z = \frac{cB_z}{4\pi a}\left(\alpha_2\frac{\partial\xi_x}{\partial z}+\alpha_3 k_0\xi_y\right)\sin\theta. \tag{43}$$

Likewise, the $\cos\theta$-dependent current perturbation is

$$\delta j_z = \frac{cB_z}{4\pi a}\left(-\alpha_2\frac{\partial\xi_y}{\partial z}+\alpha_3 k_0\xi_x\right)\cos\theta. \tag{44}$$

3. The boundary condition

The reaction of the sheath to the current perturbation of the $\sin\theta$ dependence is illustrated in Fig. 6: by applying the sheath current-voltage characteristic (38), one sees that the "upper" part of the plasma cross section is charged positively with respect to the "lower" part, giving rise to the electric field with a general direction antiparallel to the axis y, as shown in the figure. From Eqs. (38) and (43) one finds

$$E_y = -\frac{\alpha_2}{\alpha_1}\frac{cT_eB_z}{4\pi a^2e^2nu}\left(\frac{\partial\xi_x}{\partial z}+\frac{\alpha_3}{\alpha_2}k_0\xi_y\right). \tag{45}$$

Likewise, for the x component of the electric field, one finds from Eqs. (38) and (44),

$$E_x = \frac{\alpha_2}{\alpha_1}\frac{cT_eB_z}{4\pi a^2e^2nu}\left(\frac{\partial\xi_y}{\partial z}-\frac{\alpha_3}{\alpha_2}k_0\xi_x\right). \tag{46}$$

The tangential electric field gives rise to the drift of the column imprint over the surface of the endplate:

$$\frac{\partial\boldsymbol{\xi}}{\partial t} = c\frac{\boldsymbol{E}\times\boldsymbol{B}}{B^2}. \tag{47}$$

Switching to the complex representation (9), for perturbations proportional to $\exp(-i\omega t)$, one finds from Eqs. (45)–(47) the following boundary condition:

$$\eta|_{z=L} = -\kappa\frac{iv_A}{\omega}\left(\frac{\partial\eta}{\partial z}+ik_0\frac{\alpha_3}{\alpha_2}\eta\right)\Bigg|_{z=L}, \tag{48}$$

where

$$\kappa = \frac{\alpha_1}{\sqrt{2}\alpha_2}\frac{c_s}{u}\left(\frac{c}{a\omega_{pi}}\right)^2\sqrt{\beta_e} \tag{49}$$

is a dimensionless coefficient characterizing the role of the sheath resistance. The notation is

$$c_s = \sqrt{\frac{T_e}{m_i}}; \quad \beta_e = \frac{8\pi n T_e}{B_z^2}. \tag{50}$$

Again, the presence of the numerical coefficients α (which we cannot evaluate better than within a factor of 2 or so) points at the phenomenological nature of our model.

The second term on the rhs of Eq. (48), related to the displacement of the footpoint, may be affected by a radial nonuniformity of the initial state of the surface of the endplate (e.g., a higher secondary emission coefficient near the unperturbed axis). This contribution will, however, have the same azimuthal structure as the one described by Eqs. (43) and (44) and can therefore be lumped into the phenomenological coefficient α_3.

We will consider in more detail a special case where $\alpha_2=2\alpha_3$, so that

$$\eta|_{z=L} = -\kappa\frac{iv_A}{\omega}\left(\frac{\partial\eta}{\partial z}+\frac{ik_0}{2}\eta\right)\Bigg|_{z=L}. \tag{48'}$$

The relationship $\alpha_2=2\alpha_3$ is by no means universal, although it seems to represent reasonably well some of the experiments, e.g., 3. It is of particular interest, since, in the limit of a very high sheath resistance ($\kappa\to\infty$), it gives rise to the boundary condition (19) of the "perfect sliding," whereas in the limit of a zero sheath resistance we return to the boundary condition (18) of the perfect line tying. On the other hand, we understand that the ratio α_2/α_3 can be different from what we have assumed. To provide a glimpse into what can happen in such a case, we consider also a BC corresponding to a thinner skin layer, where one has $\alpha_2 \gg \alpha_3$, and the term proportional to α_3 can be completely neglected, so that

$$\eta|_{z=L} = -\kappa\frac{iv_A}{\omega}\left.\frac{\partial\eta}{\partial z}\right|_{z=L}. \tag{51}$$

In the limit of a high sheath resistivity, $\kappa \gg 1$, this model gives rise to the boundary condition (34).

As the order-of-magnitude estimates used in the derivation may lead to a sign error, one has to calibrate the sign from the condition that, in the case of no current, the sheath resistance should cause the damping of the standing Alfvén wave. The sign presented in Eqs. (48) and (48′) satisfies this condition.

We emphasize that we consider only a mode of a global displacement, where each cross section is simply shifted in the lateral direction (Fig. 2). In the case of small-scale perturbations, the presence of the sheath boundary condition may give rise to quite a potent instability driven mostly by the radial gradient of the electron temperature.[17] We do not consider these small-scale modes, which, if present, can determine the magnitude of the anomalous transport in our problem.

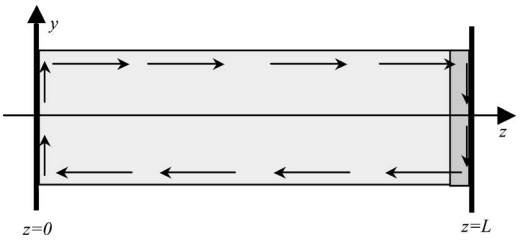

FIG. 7. The current circuit corresponding to the current pattern shown in Fig. 6. The current flows in the opposite directions at the opposite sides of the plasma column (shown in light gray) and is closed through the plasma sheath (shown in dark gray) and over the surface of the perfectly conducting electrodes. The only resistive element in this circuit is the sheath.

Equation (48) is written in such a manner that, for the typical values of ω and k, ($\omega\sim\pi v_A/L, k\sim\pi/L$), the rhs of Eq (48), aside from the coefficient κ, is of order one. The meaning of the parameter k can be understood in the following way. Consider the time of the resistive damping of the current in the circuit shown in Fig. 7. The sheath resistance is the ratio of $\delta\varphi$ to $\pi a^2\,\delta j_z$ and, according to Eq. (38), is $\sim T_e/\pi a^2 e^2 nu$, whereas the inductance of the circuit (in the CGS-Gaussian system of units) is $\sim L/c^2$. Accordingly, the inductive decay time is $\sim\pi a^2 e^2 nuL/c^2 T_e$. The ratio of the Alfvén transit time L/v_A to this damping time forms the parameter $\kappa\sim(c_s/u)(c^2/a^2\omega_{pi}^2)\sqrt{\beta_e}$. For the typical parameters of the RSX experiment[3] ($a\sim 2$ cm, $T_e\sim 10$ eV, $n\sim 10^{13}$ cm^{-3}, $B\sim 100$ G, $u/c_s\sim 1$), one has $\kappa\sim 15$.

The dispersion relation for the boundary condition (48′) is [see Eqs. (21) and (22)]

$$\tan\left(L\sqrt{\frac{k_0^2}{4}+\frac{\omega^2}{v_A^2}}\right) = -\frac{i\kappa v_A}{\omega}\sqrt{\frac{k_0^2}{4}+\frac{\omega^2}{v_A^2}}. \tag{52}$$

It may have an aperiodic (exponentially growing) root, $\omega = i\Gamma$, with Γ real. Introducing the dimensionless variables (denoted by an overcaret) via the equation

$$\hat{k}_0 = k_0 L, \quad \hat{\Gamma} = \frac{\Gamma L}{v_A}, \tag{53}$$

one obtains

$$\tan\sqrt{\frac{\hat{k}_0^2}{4}-\hat{\Gamma}^2} = -\frac{\kappa}{\hat{\Gamma}}\sqrt{\frac{\hat{k}_0^2}{4}-\hat{\Gamma}^2}. \tag{54}$$

It is easy to see that the unstable root is present if

$$k_0 > \frac{\pi}{L} \tag{55}$$

(i.e., at $I > I_{KS}/2$). In other words, the stability boundary is the same at any value of the parameter κ, starting from very small values corresponding to an almost perfect line tying. However, for $\kappa \ll 1$, the growth rate for $k_0 < 2\pi/L$ is small; if $\kappa \ll 1$, the growth rate becomes substantial only at $k_0 > 2\pi/L$. This is illustrated by Fig. 8.

It is also of some interest to see what happens to the dispersion relation (48) in the case corresponding to the boundary condition (51), i.e., to the assumption that the cur-

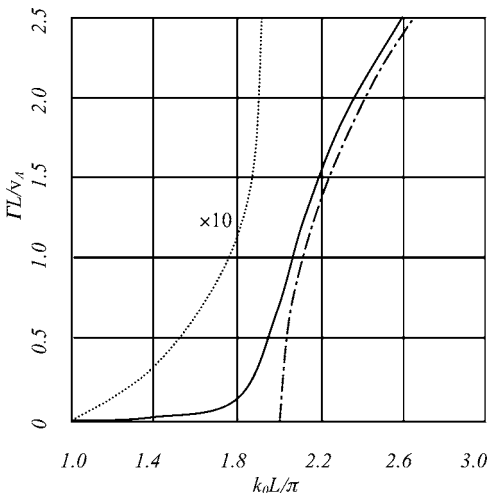

FIG. 8. The growth rate versus the parameter k_0 for a small value of κ, $\kappa=0.02$. This value corresponds to almost complete line tying, but a weak instability is present even at $k_0<2\pi/L$. The dash-dotted line corresponds to the case of a perfect line tying, when $\kappa=0$.

rent perturbation at $z=L$ is proportional to $\partial\eta/\partial z$, without the term proportional to $k_0\eta$. In this case the dispersion relation becomes

$$\tan\left(L\sqrt{\frac{k_0^2}{4}+\frac{\omega^2}{v_A^2}}\right)=-\frac{i\kappa v_A}{\left(\omega+\kappa\frac{v_A k_0}{2}\right)}\sqrt{\frac{k_0^2}{4}+\frac{\omega^2}{v_A^2}}. \quad (56)$$

At small κ (or k_0) one recovers dispersion relation (52), whereas at large κ one obtains dispersion relation (35).

IV. EFFECTS OF AN AXIAL FLOW

We now include in our model the parallel plasma flow. We will characterize it by the velocity v averaged over the cross section. The way that allows one to obtain the modified eigenequation is to switch to the frame where the unperturbed plasma is at rest. In that frame one recovers Eq. (10). After that, one switches back to the laboratory frame, using the Galilean transformation. This is equivalent to replacing an operator $\partial/\partial t$ by an operator $\partial/\partial t+v\partial/\partial z$ Equation (10) is, accordingly, replaced by

$$\left(\frac{\partial}{\partial t}+v\frac{\partial}{\partial z}\right)^2\eta=v_A^2\left(\frac{\partial^2\eta}{\partial z^2}+ik_0\frac{\partial\eta}{\partial z}\right), \quad (57)$$

where v_A is defined by Eq. (12). For the perturbations of the $\exp-i(\omega t-kz)$ type, one finds

$$(\omega-k\mathrm{v})^2=v_A^2(k^2+k_0 k), \quad (58)$$

or

$$k^2(1-M^2)+k\left(k_0+2M\frac{\omega}{v_A}\right)-\frac{\omega^2}{v_A^2}=0, \quad (59)$$

where

$$M=\frac{v}{v_A} \quad (60)$$

is the Alfvén Mach number. From Eq. (59), we obtain

$$k_{1,2}=\frac{-2M\frac{\omega}{v_A}-k_0\pm\sqrt{\left(2M\frac{\omega}{v_A}+k_0\right)^2+4\frac{\omega^2}{v_A^2}(1-M^2)}}{2(1-M^2)}. \quad (61)$$

We will limit ourselves to the analysis for the two "ideal" boundary conditions (18) or (19). For the case of the perfect line tying, substituting $k_{1,2}$ from Eq. (61) into solution (22), and imposing the boundary condition (18), we find

$$\omega^2+\omega M k_0 v_A+v_A^2\left[\frac{k_0^2}{4}-\left(\frac{n\pi}{L}\right)^2(1-M^2)^2\right]=0. \quad (62)$$

The instability criterion is

$$k_0>\frac{2\pi}{L}\sqrt{1-M^2} \quad (63)$$

(we assume that $v<v_A$). In terms of the current, the instability criterion reads as

$$I>I_{KS}\sqrt{1-M^2}. \quad (64)$$

The growth rate is

$$\mathrm{Im}\ \omega=\frac{\pi v_A}{L}\sqrt{1-M^2}\sqrt{\frac{I^2}{I_{KS}^2}-(1-M^2)}. \quad (65)$$

The real frequency is nonzero:

$$\mathrm{Re}\ \omega=-\frac{\mathrm{v}B_\varphi}{2aB_z}=-\frac{\pi\mathrm{v}}{L}\frac{I}{I_{KS}}. \quad (66)$$

As the mode under consideration is, azimuthally, the $m=1$ mode, this frequency is a rotation frequency of the perturbation. (To avoid a possible misunderstanding, we emphasize that this is an "orbital" motion, in which the center of the every slice of the plasma column rotates around the z axis; this is not a "proper" rotation of the unperturbed plasma.) The rotation frequency does not vary along the column length. For v positive (directed from $z=0$ to $z=L$), the helix screws into the $z=L$ electrode, independently of the direction of the z component of the magnetic field. Note that the frequency is nonzero at the stability margin. When we go beyond the stability margin, the rotation frequency increases.

Beyond the stability margin, the axis of the plasma column is wound over the surface that is different from (28). Now it is

$$R\equiv\sqrt{\xi_x^2+\xi_y^2}=\left(\exp\frac{zv\ \mathrm{Im}\ \omega}{v_A^2-v^2}\right)\left(\sin\frac{\pi z}{L}\right). \quad (67)$$

Note that this surface does not possess symmetry with respect to the $z=L/2$ plane. The perturbation is "skewed" in the direction of flow [Fig. 4(a), dashed line].

Consider now the stability margin in the case of the boundary condition (19), i.e., $\kappa\to\infty$. An inspection of Eq. (29) shows that the stability boundary corresponds to

$$k_0=\frac{\pi}{L}\sqrt{1-M^2}, \quad (68)$$

or

$$\frac{I_{\rm crit}}{I_{\rm KS}}=\frac{\sqrt{1-M^2}}{2}. \tag{69}$$

The parameters k_1 and k_2 that enter the eigenfunction (22) are (at the stability boundary)

$$k_1=\frac{k_0}{2}\left(\frac{1}{\sqrt{1-M^2}}-1\right);\quad k_2=-\frac{k_0}{2}\left(\frac{1}{\sqrt{1-M^2}}+1\right). \tag{70}$$

The rotation frequency of the mode is

$$\omega=-\frac{\pi v}{L}\sqrt{1-M^2}, \tag{71}$$

with the helix screwing into the $z=L$ electrode. The surface over which the axis of the perturbed plasma column is wound is still the same as (33).

We do not present here a lengthy analysis of Eq. (29) for supercritical currents and just note that, in the supercritical domain with the flow present, the surface (33) gets skewed in the direction of the flow, as sketched in Fig. 4(b), dashed line.

V. THE EFFECTS OF BULK RESISTIVITY

Now we switch to the effects of the bulk plasma resistivity. When bending of the plasma column occurs, the initially uniform axial magnetic field is perturbed, generating the restoring force, which, in the limit of a perfect conductivity, is described by the first term on the rhs of Eq. (58). In the case of a finite conductivity, the currents and magnetic field perturbations induced by the motion of the column become smaller due to resistive effects. This leads to a decrease of the restoring force. Finally, in the limit of a very low conductivity, the axial magnetic field is not perturbed at all (remains uniform) and the restoring force vanishes.

To include these effects in the phenomenological model, one can use the induction equation for the perturbation $\delta\boldsymbol{B}$ of the initially axial magnetic field. One has

$$\delta\dot{\mathbf{B}}=B_z\frac{\partial\xi}{\partial z}-\frac{\delta\mathbf{B}}{\tau_r}. \tag{72}$$

Here we introduced the resistive time τ_r for a phenomenological characterization of the resistive dissipation of $\delta\boldsymbol{B}$:

$$\tau_r=\frac{2\pi a^2\sigma}{c^2}, \tag{73}$$

where σ is the parallel electrical conductivity of the plasma. [The current generated by the tilts of the column is an axial current; see Eq. (42).] Note that, in the spirit of the phenomenological approach, we do not solve the problem of the magnetic field diffusion, just introduce a characteristic time τ_r. For the perturbations of the form of $\exp(-i\omega t+ikz)$ one can rewrite Eq. (72) as

$$\delta\boldsymbol{B}=\frac{i(\omega-kv)\tau_r}{i(\omega-kv)\tau_r-1}ikB_z\boldsymbol{\xi}. \tag{74}$$

The restoring force caused by the deformation of the axial magnetic field is proportional to $\delta\boldsymbol{B}$. Accordingly, one has to replace the first term on the rhs of Eq. (58) by

$$\frac{i(\omega-kv)\tau_r}{i(\omega-kv)\tau_r-1}k^2v_{\rm A}^2\eta. \tag{75}$$

Now we consider the last term in Eq. (58), which describes the interaction of the tilted current with the external magnetic field. Here the situation is quite different, because the axial current is sustained by the applied voltage and does not decay due to resistive effects. When the filament becomes wavy, the current just follows the filament. Consider as an example the case where the electrical conductivity is so low that the axial magnetic field is not perturbed at all (remains uniform). Then the force acting per unit length of the column can be presented simply as

$$\frac{B_z}{c}[\boldsymbol{I}\times\boldsymbol{e}_z]=\frac{B_zI}{c}\left(\boldsymbol{e}_x\frac{\partial\xi_y}{\partial z}-\boldsymbol{e}_y\frac{\partial\xi_x}{\partial z}\right), \tag{76}$$

where $\boldsymbol{I}$ is a vector collinear to the tilted axis of the column, and $|\boldsymbol{I}|$ equals the unperturbed current; $\boldsymbol{e}_{x,y,z}$ are the unit vectors parallel to the coordinate axes. This is exactly the same force as in Eq. (7), which corresponds to the perfect conductivity. We see that, in the limiting cases of very high and very low conductivity, the force term associated with the axial current remains the same. This is not a coincidence: one can show that, in the intermediate case of a finite conductivity, the force still remains the same as in the two limiting cases. This can be proven by integrating the Maxwell stress tensor over the surface situated at a distance r such that $a\ll r\ll 1/k$, where the magnetic field is just a superposition of a uniform axial field and the field of a tilted current filament.

Collecting Eqs. (58), (75), and (76), one finds the following model equation corresponding to the finite plasma resistivity:

$$(\omega-kv)^2=v_{\rm A}^2\left(\frac{i(\omega-kv)\tau_r}{i(\omega-kv)\tau_r-1}k^2+k_0k\right). \tag{77}$$

Note that, for a nonzero flow velocity, the equation for k becomes of the third order, thereby requiring the imposition of one more boundary condition. This would be the condition that $\delta\boldsymbol{B}$ is zero at $z=0$ (the finite-conductivity fluid cannot carry a current sheath, and enters the volume in question without any initial perturbation of the magnetic field). Implementing this boundary condition in the general case is quite an onerous task. The boundary condition at $z=L$ also becomes quite complex.

The dimensionless parameter that characterizes the role of resistive effects is

$$\zeta=\frac{\pi v_{\rm A}\tau_r}{L} \tag{78}$$

(this is a product of the characteristic frequency and the resistive time). For the parameters of the RSX experiment ($L\sim 100$ cm, $a\sim 2$ cm, $T_e\sim 10$ eV, $n\sim 10^{13}$ cm^{-3}, $B\sim 100$ G), one has $\zeta\sim 6$.

The main role of the resistive effects is related to the decrease of the critical current. Equation (79) below shows that slow-enough perturbations in a nonflowing plasma would become unstable, even at the current substantially lower than the KS current. In other words, if resistive modes

are considered, a "hard" stability limit is replaced by a gradual emergence of the slow modes, which begin to show up at relatively low currents. The addition of the flow, however, leads to at least partial stabilization of these modes. All these effects are encapsulated in relatively simple (algebraic!) equations of our phenomenological model.

To illustrate the effect of a finite resistivity, let us consider the case where the parameter ζ [Eq. (77)] is very small (small τ_r). We assume also that the flow is absent, $v=0$. In this case there appears a possibility of the formation of a continuous spectrum of unstable modes, even at the current significantly less than the KS current. Indeed, in the limit of a zero τ_r, Eq. (77) yields

$$\omega^2 = v_A^2 k_0 k. \tag{79}$$

Clearly, for the "negative" handedness of the perturbation (such that $k_0 k<0$), perturbations are unstable, with the growth rate

$$\mathrm{Im}\ \omega = v_A \sqrt{|k_0 k|}. \tag{80}$$

The nature of the mode is as follows. At a high plasma resistivity, the strong axial magnetic field is not frozen into the plasma anymore, and a helical perturbation of the appropriate handedness experiences an imbalanced radial force that leads to its growth.

In order to be able to form localized perturbations insensitive to the boundary conditions, we have to assume that $k \gg \pi/L$. Still, the growth rate must be slow enough, so that the condition $Im\ \omega\tau_r \ll 1$ holds. These two constraints are compatible with each other, provided the condition

$$\varsigma^2 \frac{I}{I_{KS}} \ll 1 \tag{81}$$

is satisfied. In other words, at a small enough plasma current the instability can be present at even relatively high values of ζ (relatively high conductivity). However, the instability in this case is quite slow, with the *e*-folding time longer than the resistive time. Therefore, these perturbations will be sensitive to the presence of the plasma flow and will be advected toward the $z=L$ endplate. At $\zeta \gg 1$, this requires a relatively low flow velocity,

$$v > \frac{\tau_r L}{\pi}, \tag{82}$$

i.e., $M>1/\zeta$.

An interesting feature of the situation with $\zeta \sim 1$ is the fact that the perturbation will have a substantial real frequency, even if there is no flow.

VI. DISCUSSION

The phenomenological approach developed in our paper allows one to study the stability of a long-thin plasma column with a number of effects accounted for in a unified manner. Those effects include the presence of the axial boundaries, axial plasma flow, sheath resistance, and the bulk plasma resistance. We have presented several examples of incorporating some of these effects into an actual analysis.

An important assumption of our model is that there is a boundary beyond which the plasma electrical conductivity essentially vanishes, so that the column is surrounded by a vacuum. We, therefore, will not be able to consider the situations where there is a conducting medium outside the column. One more constraint stems from our assumption that the axial wavelength of the perturbation is much longer than the column radius.

With these assumptions made, the description of the column deformations becomes quite simple: we characterize them just by rigid lateral displacements of the plasma slices [Eq. (4)]. (With that, we of course, abandon any attempts of describing internal kinks; on the other hand, description of the external kink becomes quite efficient.)

The theory developed in this paper is linear. Strictly speaking, this does not allow us to consider the plasma dynamics at the axial current substantially exceeding the threshold. However, the general structure of the perturbation determined by a linear eigenfunction should be quite a robust entity and thereby gives a hint on the shape of the column in the nonlinear regime. A weakly nonlinear theory of the type suggested in Ref. 11, but with the effects of the plasma flow and sheath resistance included, should be feasible.

ACKNOWLEDGMENT

This work was performed for the US DOE by UC LLNL under Contract No. W-7405-Eng-48.

[1] J. P. Freidberg, *Ideal Magnetohydrodynamics* (Plenum, New York, 1987).
[2] P. M. Bellan, Phys. Plasmas **12**, 58301 (2005).
[3] I. Furno, T. P. Intrator, E. W. Hemsing, S. C. Hsu, S. Abbate, P. Ricci, and G. Lapenta, Phys. Plasmas **12**, 55702 (2005); I. Furno, T. Intrator, E. Torbet, C. Casey, M. D. Cash, J. K. Campbell, W. J. Fienup, C. A. Werley, and G. A. Wurden, Rev. Sci. Instrum. **74**, 2324 (2003).
[4] D. D. Ryutov, R. H. Cohen, and L. D. Pearlstein, Phys. Plasmas **11**, 4740 (2004).
[5] C. C. Hegna, Phys. Plasmas **11**, 4230 (2004).
[6] A. W. Hood, Plasma Phys. Controlled Fusion **34**, 411 (1992).
[7] S. I. Braginski, in *Reviews of Plasma Physics*, edited by M. A. Leontovich (Consultants Bureau, New York, 1965), Vol. 1, p. 205.
[8] T. B. Kaiser, W. Nevins, and L. D. Pearlstein, Phys. Fluids **26**, 351 (1983).
[9] M. D. Kruskal and J. L. Tuck, Proc. R. Soc. London, Ser. A **A245**, 222 (1958); M. D. Kruskal, J. L. Johnson, M. B. Gottlieb, and L. M. Goldman, Phys. Fluids **1**, 421 (1958).
[10] V. D. Shafranov, At. Energ. **5**, 38 (1956).
[11] I. M. Lanskii and A. I. Shchetnikov, Sov. J. Plasma Phys. **16**, 322 (1990).
[12] I. B. Bernstein, E. A. Frieman, M. D. Kruskal, and R. M. Kulsrud, Proc. R. Soc. London, Ser. A **A244**, 17 (1958).
[13] P. Stangeby, *The Plasma Boundary of Magnetic Fusion Devices* (IoP, Bristol, 2000), p. 81.
[14] W. Kunkel and J. Guillory, in *Phenomena in Ionized Gases*, Proc. 7th Conf. Belgrade, 1965, Gradjevinska Knjiga, Belgrade, Yugoslavia, 1966, Vol. 2, p. 702.
[15] B. B. Kadomtsev, in *Phenomena in Ionized Gases*, Proc. 7th Conf. Belgrade, 1965, Gradjevinska Knjiga, Belgrade, Yugoslavia, 1966, Vol. 2, p. 610.
[16] D. Farina, R. Pozzoli, and D. D. Ryutov, Phys. Fluids B **B5**, 4055 (1993).
[17] H. L. Berk, D. D. Ryutov, and Yu. A. Tsidulko, JETP Lett. **52**, 23 (1990).